COMPARISONS OF MEASURED AND MODELED BRDF AND TRANSMISSION OF PREPARED PARTICULATE LAYERS

Hao Zhang and Kenneth J. Voss
hzhang@physics.miami.edu, voss@physics.miami.edu
Physics Department, University of Miami, Miami, FL 33124

INTRODUCTION

The relationship between the surface Bi-directional reflectance distribution function (BRDF) of closely packed grain layers and the optical properties of the individual particles is an important problem in many disciplines of science and engineering. In shallow water remote sensing with significant bottom BRDF effects, it would be important to understand the following questions[1-4]. How well does the radiative transfer equation (RTE) work for closely packed sediment particles? Are any single scattering features of individual grains retained when grains are touching? What are the effects of surface roughness on BRDF measurements? Can intrinsically forward scattering particles have a backscattering BRDF when aggregated? Can diffraction be ignored when grain layers have high values of the filling factor? How do analytical reflectance models such as Hapke's isotropic multiple scattering approximation (HIMSA)[5], Hapke's anisotropic multiple scattering approximation (HAMSA)[6] and the Lumme-Bowell model[7] (LB model) work in comparison with the strict RTE solutions such as the DISORT[8] and Mishchenko et. al.'s bi-directional reflection function algorithm[9] (MBRF)? To answer these questions, controlled laboratory BRDF and transmission measurements on packed surfaces of spherical particles with known optical properties have been carried out. Measurement results are compared with the 5 RTE models mentioned above.

INSTRUMENTS AND SAMPLES

A simple goniometric scattering meter was built to measure the scattering of light from packed layers. This gonio-meter uses a Mells-Griot He-Ne laser (632.8 nm-wavelength) as the light source with either p- or s-polarized incidence. The full angular resolution is 2.9°. The angular error was estimated to be less than 1.5°. The measured REFF on a Labsphere nominal 99% reflectance plaque agrees with other measurements[10] within 2% below 70° viewing angle and within about 4% above 70° viewing angle.

Two types of NIST traceable spherical particles are employed in this work: polystyrene spheres with a nominal diameter of 200 μm from Duke Scientific Corporation and silicon glass spheres with nominal diameter of 600 μm from Whitehouse Scientific. Both kinds of spheres have narrow size distributions provided by their manufacturers.

RESULTS AND DISCUSSIONS

Fig.1 shows the calculated Mie phase functions for the 200 μm and 600 μm spheres for two orthogonal polarizations.[11] There are two prominent features for both samples. First, the s-polarization has much stronger rainbow features than the p- counterpart. Second, a steep drop-off feature is present around the rainbow region. Such characteristics may be used as indications of single scattering features in scattering measurements of aggregated spheres.

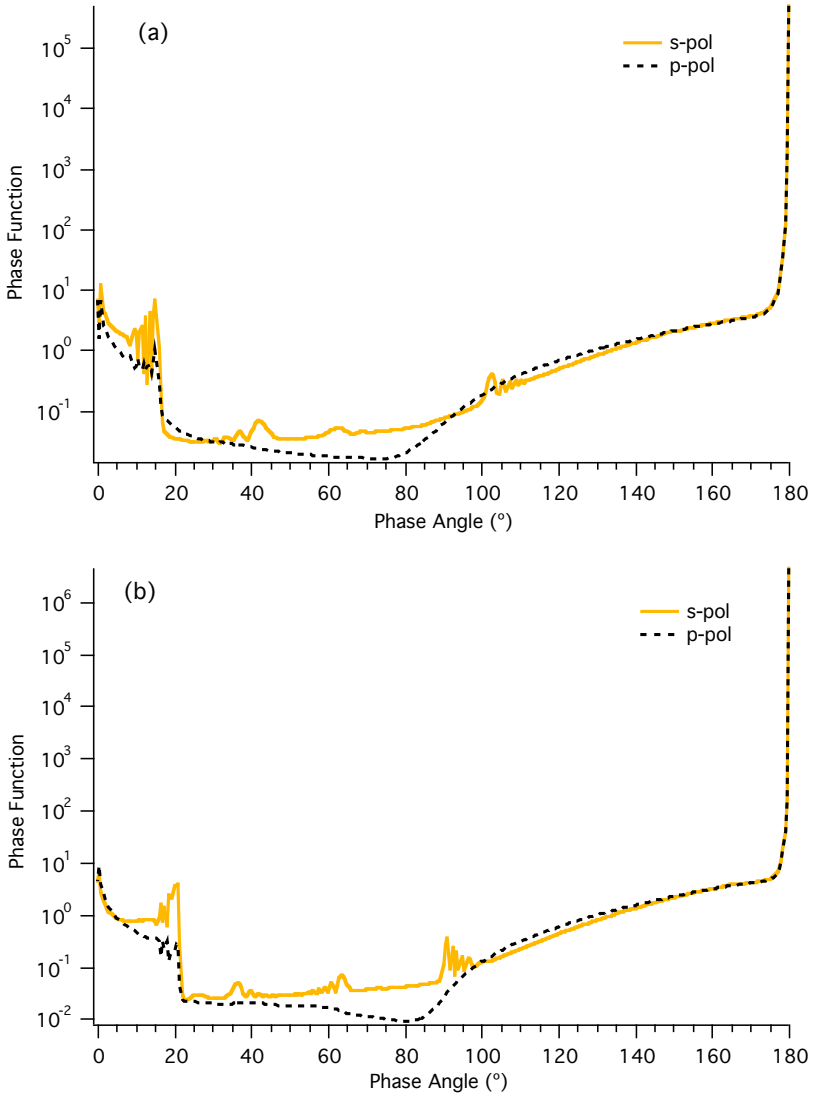

Fig. 1 Mie phase functions of (a) 200 μm and (b) 600 μm spheres. "s-pol" and "p-pol" means the electric field of incident irradiance is perpendicular and parallel to the scattering plane, respectively. The unpolarized Mie phase function is their average.

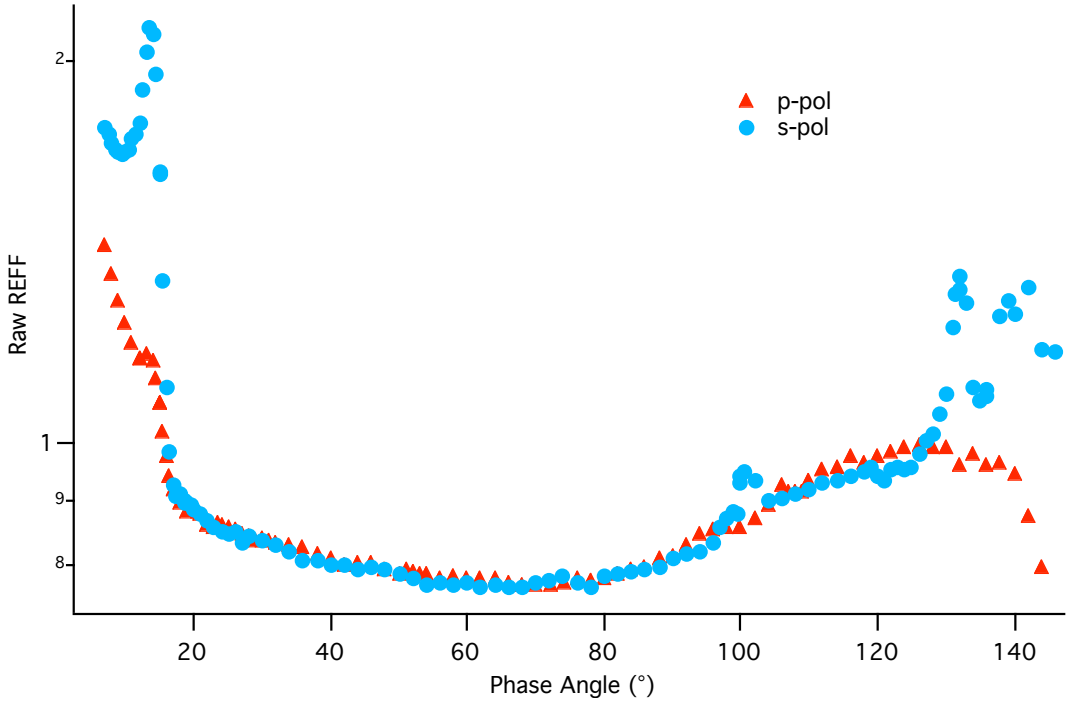

Fig. 2 Raw REFF of 200 μm 10 mm-thick 200 μm sphere layer for two orthogonal incident polarizations at -60° incidence. The viewing zenith angle in this configuration is phase angle minus 60°.

Fig. 2 shows the REFF measurements on the 200 μm sphere layers for two polarizations at 60° incidence. When compared with the Mie counterparts shown in Fig. 1(a), one can see that the reflectance curves for the two orthogonal polarizations resemble their respective Mie phase functions. Besides the strong rainbow peak that appears in the s-pol, a peak around 100° phase angle (or 40° viewing angle in this configuration) is also present. The peaks above 70° viewing angle, however, must be caused by surface roughness since they do not repeat consistently in repeated measurements with different surface realizations. The p-pol, on the other hand, exhibits only a shoulder around the rainbow region and remains featureless throughout the rest of the region, closely resembling its p-polarization phase function. It is also seen that the steep drop-off features on the larger phase angle side of the rainbow present in the Mie phase functions for both polarizations are preserved in the respective REFF. However, many of the Mie features present in s-polarizations such as the peaks around 40° phase angle disappear in the s-pol.

The comparison of the gonio-meter measurements and the RTE models are shown in Fig. 3 for the 200 μm spheres, and in Fig. 4 for the 600 μm sphere, respectively. Here the DISORT is used to represent the strict RTE solution since we have found that except within the rainbow region it agrees with MBRF very well. It can be seen that DISORT is

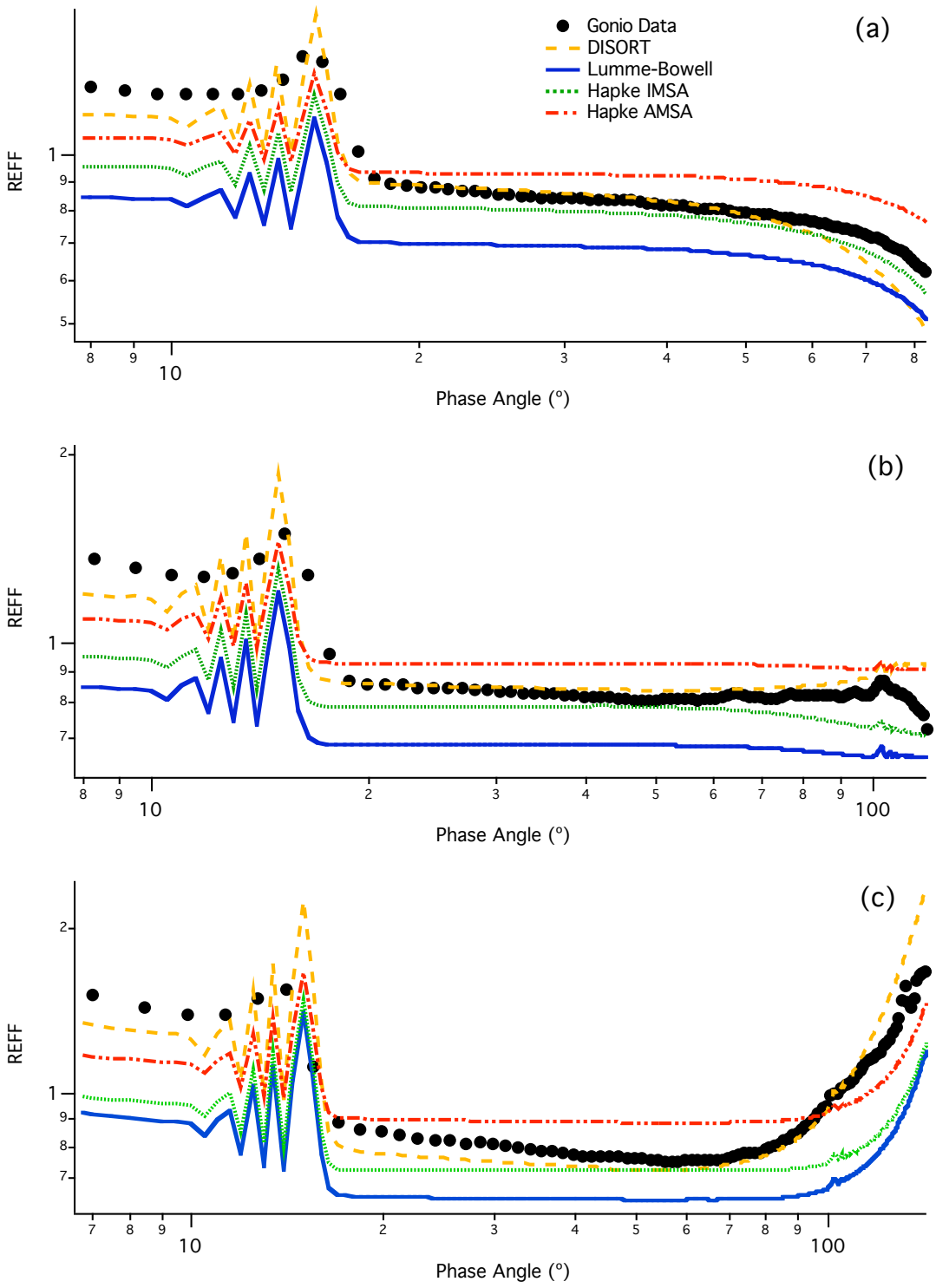

Fig. 3 Comparisons of goniometric measurement, DISORT, LB model, HIMSA and HAMSA for a 10 mm-thick (=88.5) 200 m sphere layer. Incident zenith angles are (a) 0° (b) 35° and (c) 60°.

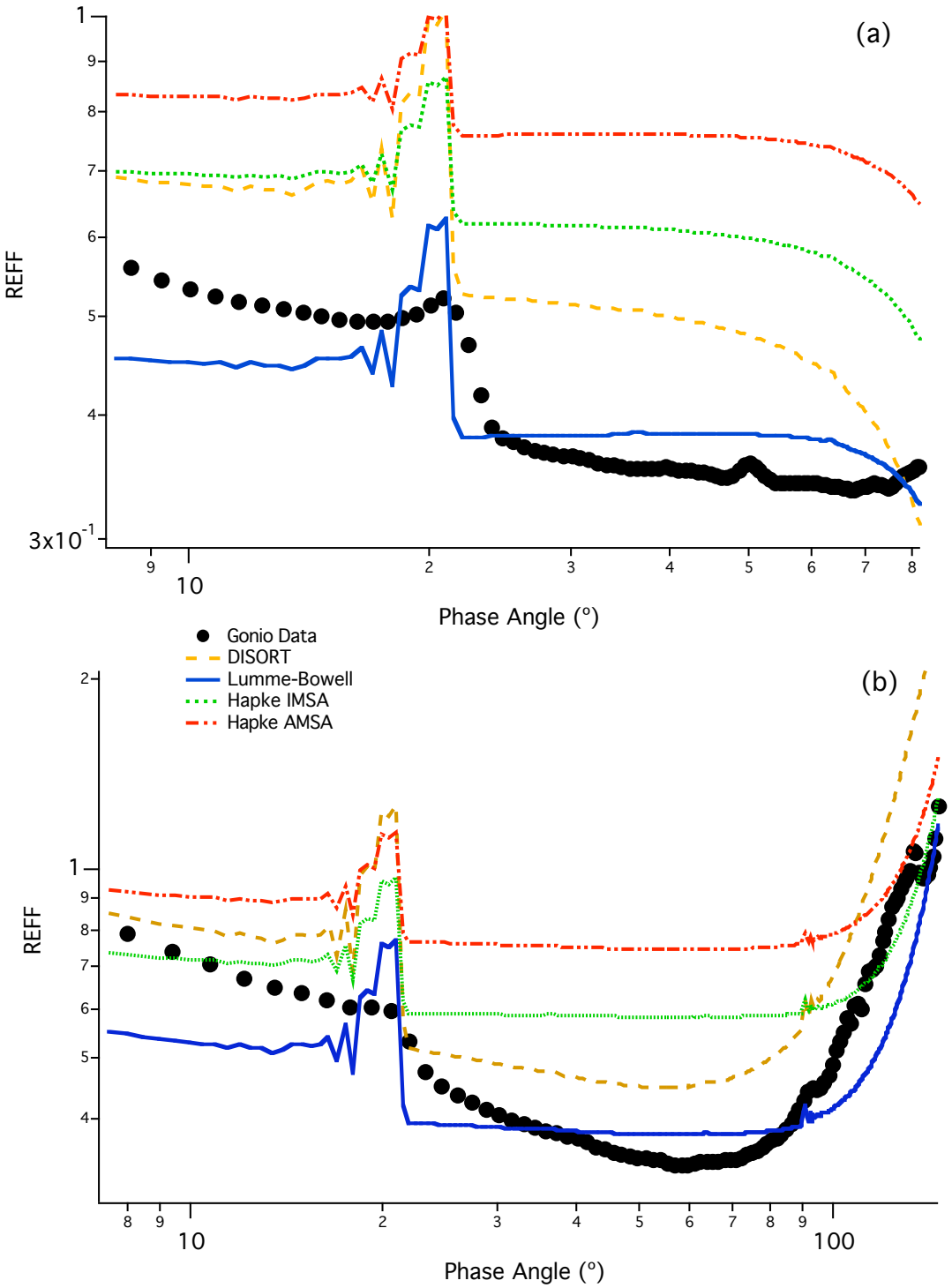

Fig. 4 Comparisons of goniometric measurement, DISORT, LB model, HIMSA and HAMSA for a 15mm-thick (=41.25) 600 m sphere layer. Incident zenith angles are (a) 0° and (b) 60°.

very close at phase angles from 15° to between 55° and 110° depending on illumination angle. The upper value beyond which DISORT either underestimates or overestimates the measured REFF is near phase angle = 55° for $\theta_i = 0^\circ$; phase angle = 70°, for $\theta_i = 35^\circ$; phase angle = 110° for $\theta_i = 60^\circ$. All three approximation models have larger errors than DISORT. Compared to the HIMSA, the improved Hapke model (HAMSA) is a better approximation in the backscattering region, but is up to 10% higher than measurements in the region where DISORT works well. The LB model is always too low in all phase angle ranges, which is caused by the similarity relation transformed albedo used in the *H* function.

In the case of the 600 μm spheres, all models other than the LB model predict much higher values than measurements. While the LB model appears to make the best prediction, in the 200 μm sphere case the LB model was shown to have a multiple scattering part that was too low. The huge difference between the data and DISORT could possibly be attributed to errors from (1) non-ideal condition of the 600 μm spheres; (2) incorrect estimate of single scattering albedo ω_0 or imaginary refractive index n_i. The first error source is almost certain. Visually with a 15X eyepiece, the 600 μm spheres are found to include quite a few non-spherical grains including spheroids, broken spheres, and even some that appeared colored. This could also be deduced from the data (Fig. 4) where the rainbow feature is small at normal incidence and basically does not exist at 60°-incidence, indicating the 600 μm spheres either contain many non-spherical grains or have larger absorption than estimated. For the second possible error, although in principle one can run the Mie code and then DISORT with various trial combinations of n_i and ω_0 to find the best values to fit the data, it is not helpful from the predictive point of view. The estimated filling factor 0.54 for this sample is well below the lower limit of the typical RCP value 0.6, thus the sampled scattering volume might not be statistically big enough and local packing structures could effect the scattering patterns. In fact we have found the 600 μm spheres have larger sample-to-sample variations than the 200 μm spheres in repeated measurements. More experimental results are needed to answer these questions.

Effects of multiple scattering

Fig. 5 shows the REFF of the measurement data for the 10 mm-thick layer and the single scattering approximation for the 200 μm spheres at three incident angles. It can be seen that the single scattering contribution is several tens of percent within the rainbow and drops down to a few percent outside of it. This low fraction remains quite flat until phase angle 100° (for 35° and 60° incidences) where it starts to climb to about 10% and further to nearly 70% around the grazing angle (for 60° incidence). However the REFF minimum is on the order of 80%. This may semi-quantitatively explain why, for the 200 μm spheres, the peaks in the Mie phase function around 40° phase angle have been

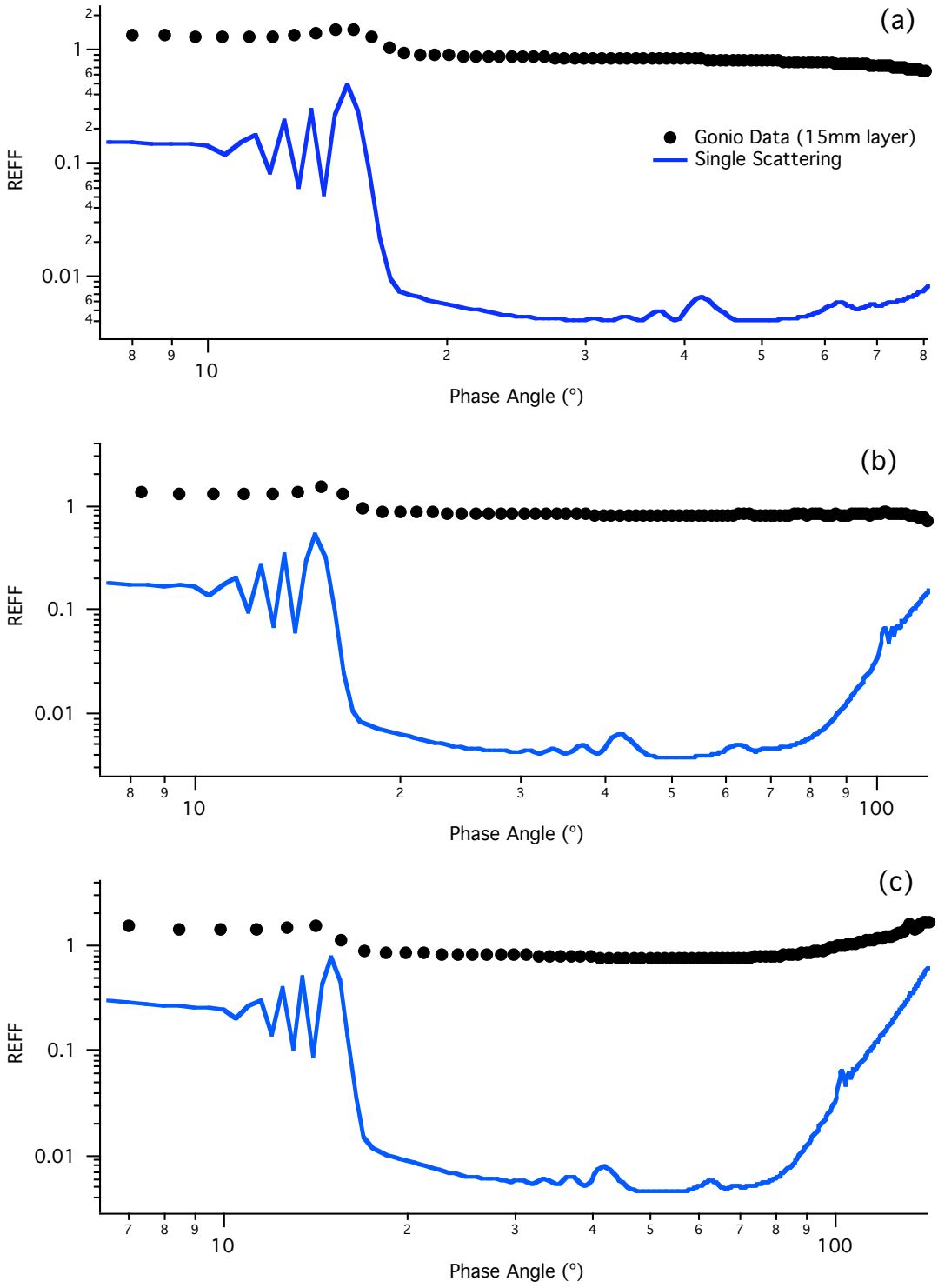

Fig. 5. Contributions of single scattering to total reflectance at (a) normal (b) 35° and (c) 60° incidence.

totally washed out while those around 100° are evident in the REFF. This also shows that since both the rainbow and the grazing regions consist of larger single scattering

contributions they are also more sensitive to surface roughness caused by packing structures.

Effects of Diffraction

Both the Hapke and LB models treat diffraction as undistinguishable from the incident flux thus the diffraction peak should be removed when using Mie phase functions. In order to evaluate the accuracy of this assumption, we performed the δ-N approximation computations to look at the diffraction removed DISORT results. Fig. 6 is the comparison of DISORT, δ-N truncated Mie phase function supplied DISORT (DISORT Delta-N) and HAMSA for the 200 μm spheres. This example demonstrates that (1) the HAMSA is a significant improvement over the HIMSA in approximating the diffraction-removed numerical RTE solution over rather large phase angle range (agrees with DISORT Delta-N). The improvement is very good in the backward direction and the overall agreement is the best at 35°-incidence. (2) Treating diffraction as un-scattered may not be a good approximation for this specific example, as HAMSA (and now DISORT Delta-N) overestimate the REFF through much of the phase angle range for the 200 μm spheres.

Surface roughness effects

For the 200 μm sample for which the predicted RTE is better, the discrepancies between DISORT and the measurements in forward scattering region could be attributed to surface roughness, as measurements in this region have the largest sample to sample variations. In this work the LB theory is chosen because the case for packed sphere surface is well documented. Since all the measurements here are on macroscopically flat surfaces, the term "roughness" only refers to microscopic roughness with scales of several particle diameters. The discussions of Fig. 5 have shown that single scattering contributes a significant amount in the forward direction thus the LB roughness correction is applied to the single scattering term only. Fig. 7 shows the comparisons of the measurements, DISORT and LB roughness corrected DISORT. At normal incidence (Fig. 7(a)) the correction has little effect. For 35° and 60° incidences although this correction factor further reduces the DISORT values in the backscattering direction, it improves the agreement in the grazing angles. Since single scattering contributes tens of percent in these two regions, applying the roughness correction to single scattering changes the intensities significantly.

The reflectance data for both samples (Fig. 3 and Fig. 4) show that during the progression from normal to oblique incidence, a peak in the forward direction shows up but is never as strong as the backscattering peak. This demonstrates that intrinsically forward scattering particles, when in aggregate, can look backscattering in reflectance measurements[1,3] thus inverting reflectance data to retrieve single scattering quantities should be done cautiously.

Even for the measurements for which the strict RTE has partial success (Fig. 3), the backscattering peaks are about 10% higher than predicted in the smallest phase angle region (~8°). Due to the mechanical interference the current gonio device can only detect

scattered radiance at phase angles larger than 7°, thus opposition effects which are normally observed in the phase angle range of 2°-7° are not detected here. This backscattering range is perhaps among the most poorly understood in radiative transfer theory, as the numerical RTE solutions do not agree with each other in this region. Neither the Hapke's hotspot function[5] or Lume-Bowell's shadowing factor[7] can predict

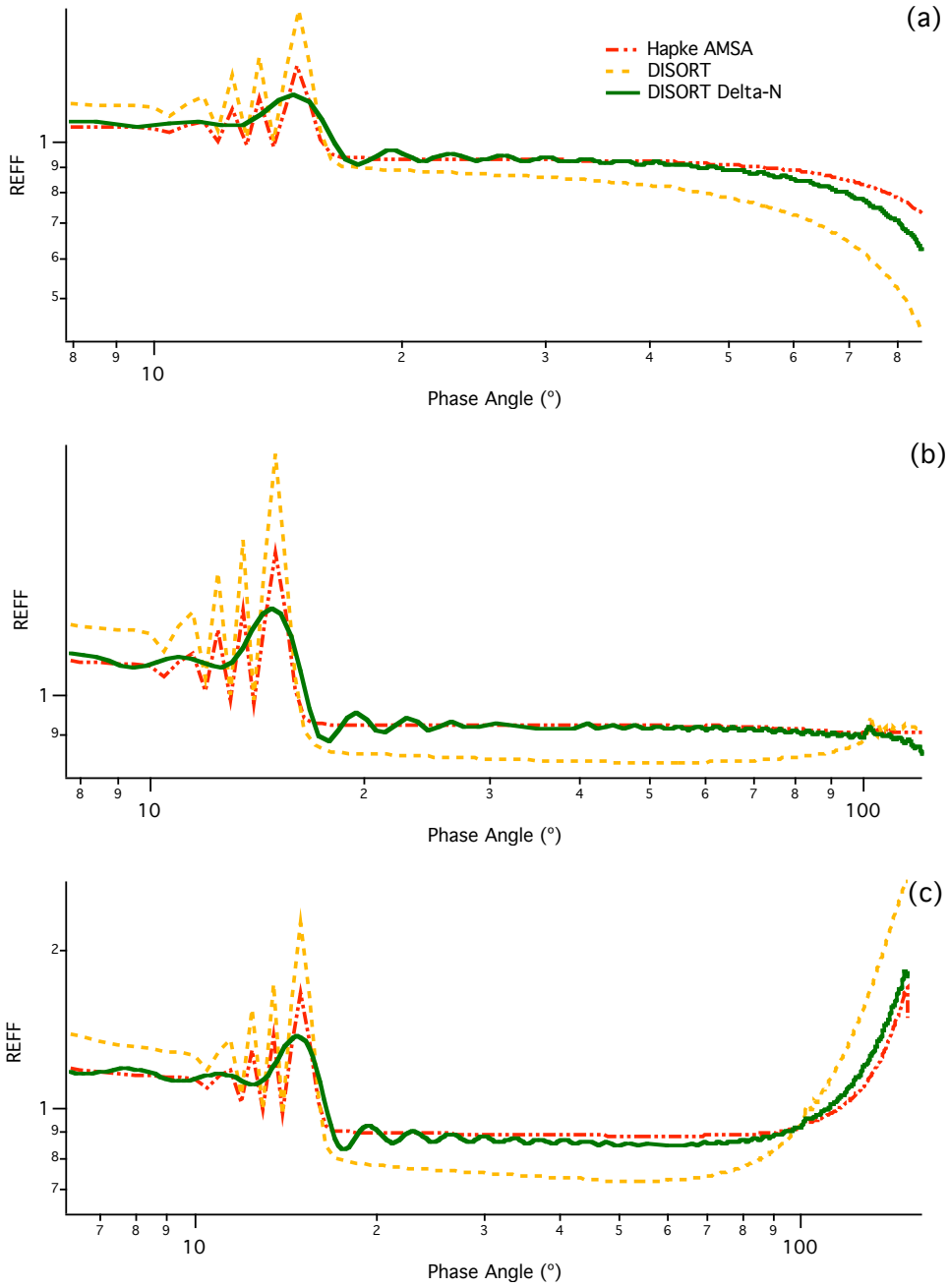

Fig. 6. Comparisons of HIMSA, HAMSA, DISORT □-N DISORT and goniometric measurement for a 10 mm-thick (□=88.5) 200 □m layer. Incident zenith angles are (a) 0° (b) 35° and (c) 60°.

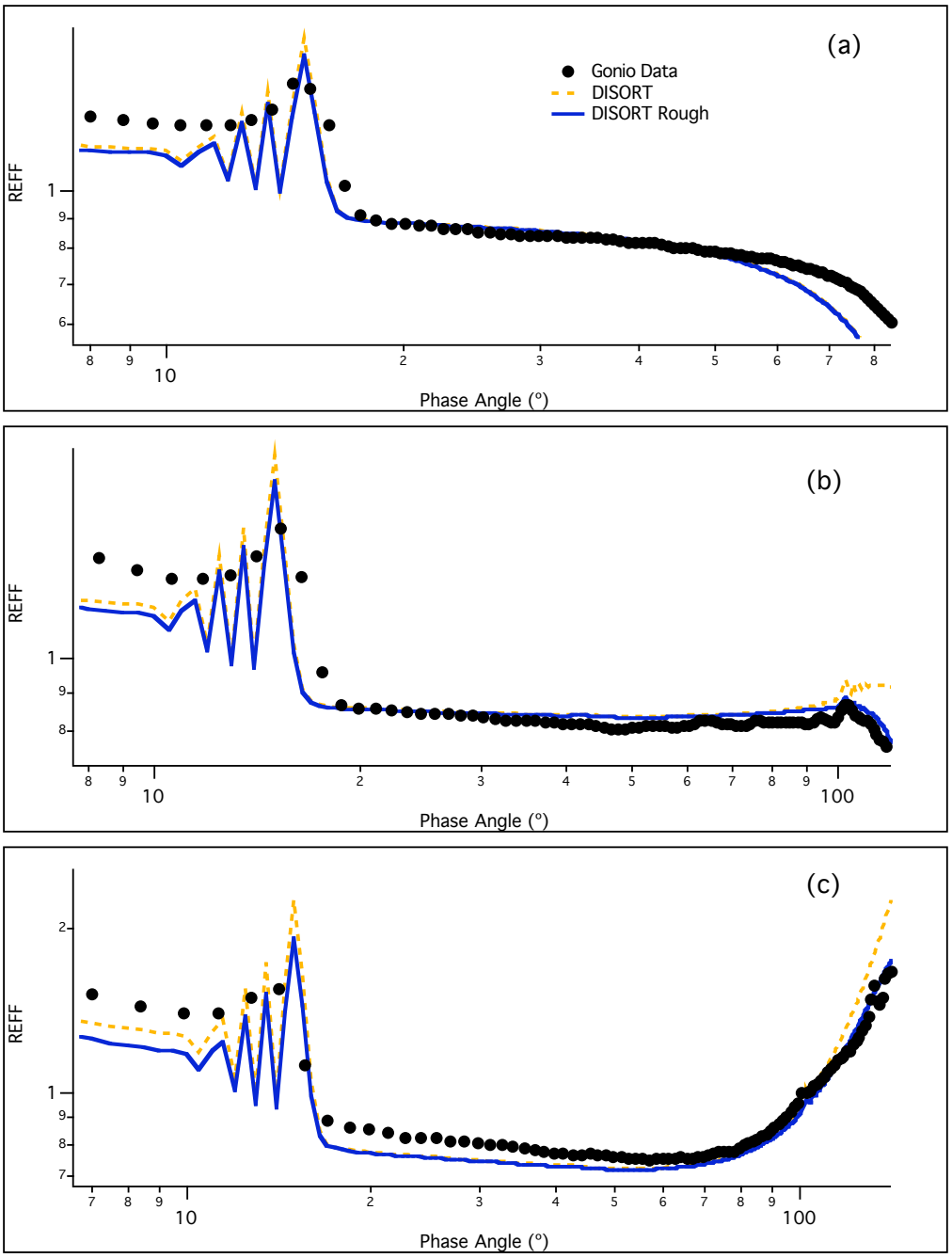

Fig. 7. Comparisons of DISROT, roughness corrected DISORT and the measurements. Incident zenith angles are (a) 0° (b) 35° and (c) 60°.

this enhancement since both are monotonously decreasing from a value of 1 at 0° phase angle (Hapke's model) or 0.5 (LB model).

Transmission Results

Fig. 8 and Fig. 9 are comparisons of DISORT and gonio transmission data with various thicknesses of the 200 μm and the 600 μm spheres, respectively. In reflectance region, the disagreement between the 600 μm spheres and RTE predictions is larger than that between the 200 μm spheres and RTE calculations. This may be explained by the same reasoning given in the reflectance results. There are several common features for both samples: measurements are better predicted by RTE (1) at oblique incidence rather than at normal; (2) for thinner layers than thicker layers; (3) in reflectance rather than in transmission. The first feature was also seen in reflectance data shown in Figure 3, and may be at least partially attributed to inappropriate optical thickness estimations. The second feature may be associated with the first, as when incident light is oblique, the penetration depth is less than normal incidence as derived by DISORT. The third one appears to be more complex to explain, as many factors like the glass slide effects and/or lack of a transmission standard may contribute to the discrepancies.

In summary, we have performed controlled laboratory BRDF measurements on NIST-traceable nearly mono-disperse sphere samples and compared these measurements with five radiative transfer models. It has been found that numerical solution of the RTE (DISORT) can predict the BRDF well over a large phase angle range especially at oblique incidence, for 200-μm diameter polymer spheres. The semi-empirical models such as the Hapke and Lumme-Bowell models predict less anisotropic scattering than the strict RTE and the measurements. When Lumme-Bowell's surface roughness correction is combined with DISORT, the REFF at oblique incidence can be very well predicted except in the backscattering direction.

Significant single scattering features are retained even when the spheres are closely packed with filling factor values higher than 0.5. However, the overwhelming multiple scattering tends to wash out some of the sharp features present in single scattering.

The current work suggests that more extensive reflectance/transmission measurements on samples with known single scattering properties are desired to further test the current scattering models. More RTE modeling efforts, especially applicable to high density media can also be appropriate. It is also anticipated that diffraction effects must be considered in order to model the particle scattering more accurately.

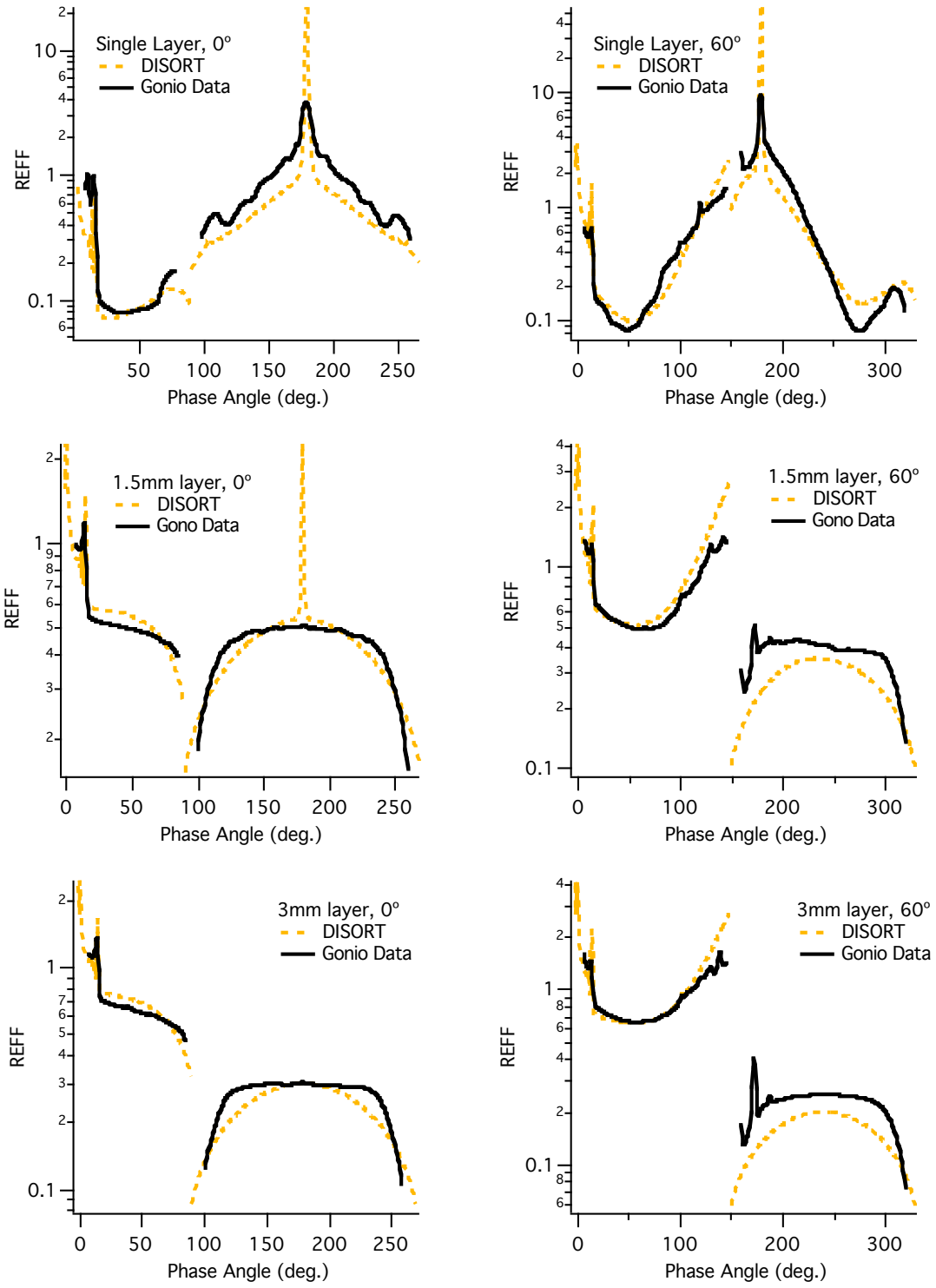

Fig. 8. DISORT and gonio data for layers of the 200 □m spheres. The layer thicknesses and incident angles are indicated in graphs.

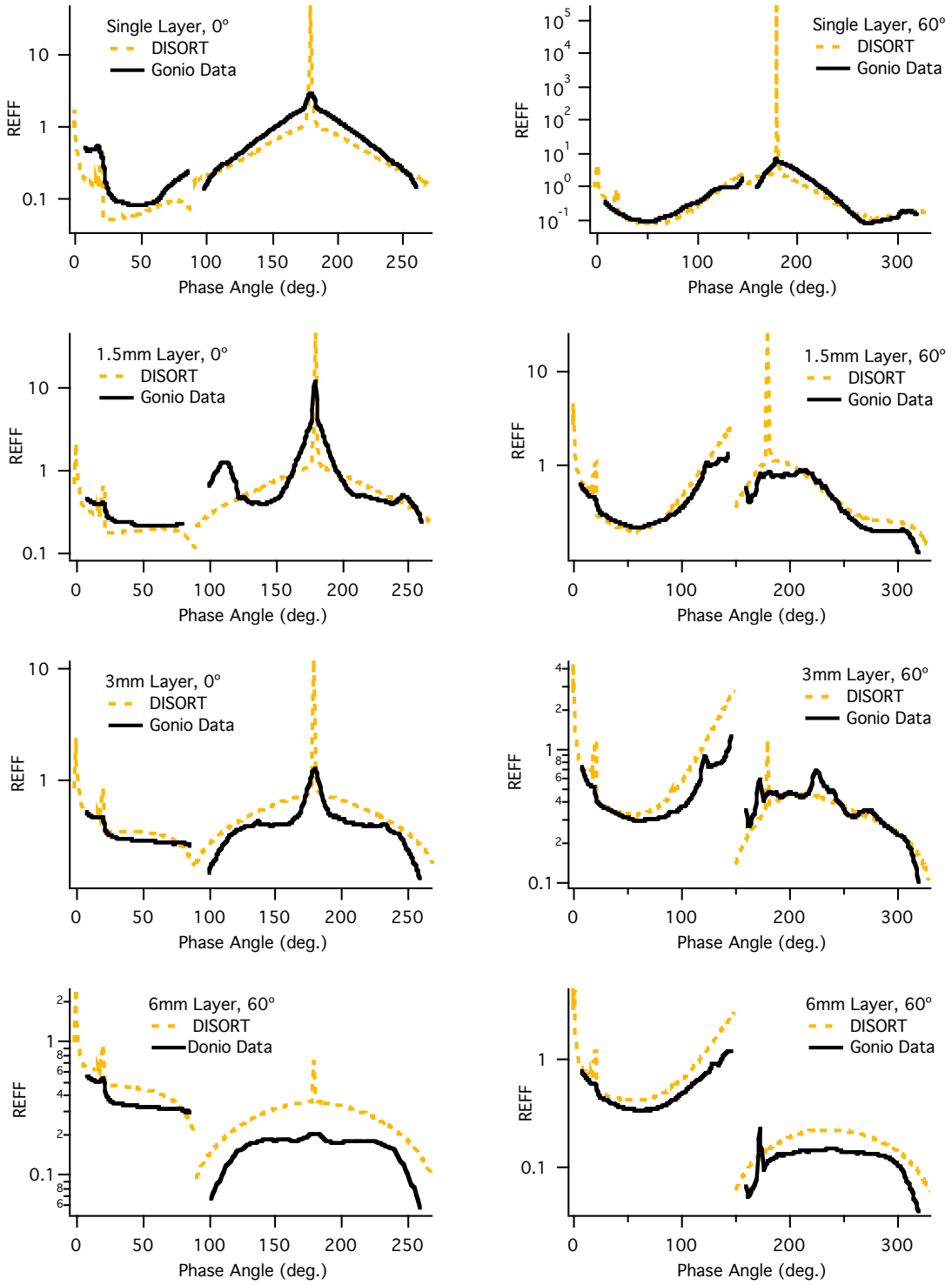

Fig. 9 DISORT and gonio data for layers of the 600 □m spheres. The layer thicknesses and incident angles are indicated in graphs.

References:

[1] M. I. Mishchenko, “Asymmetry parameters of the phase function for densely packed scattering grains,” J Quant. Spectrosc. & Radiat. Transfer 52, 95-110 (1994).

[2] B. Hapke, “Are planetary regolith particles back scattering? Response to a paper by M. Mishchenko,” J Quant. Spectrosc. & Radiat. Transfer 55, 837-848 (1996).

[3] M. I. Mishchenko and A. Macke, “Asymmetry parameters of the phase function for isolated and densely packed spherical particles with multiple internal inclusions in the geometric optics limit,” J Quant. Spectrosc. & Radiat. Transfer 57, 767-794 (1997).

[4] B. Hapke, “Scattering and diffraction by particles in planetary regoliths,” J Quant. Spectrosc. & Radiat. Transfer 61, 565-581 (1999).

[5] B. Hapke, *Theory of reflectance and emittance spectroscopy* (Cambridge Univ., New York, 1993).

[6] B. Hapke, "Bidirectional reflectance spectroscopy 5. The Coherent Backscatter Opposition Effect and Anisotropic Scattering," Icarus 157, 523-534 (2002).

[7] K. Lumme and E. Bowell, “Radiative transfer in the surfaces of atmosphereless bodies. I. Theory,” Astron. J. 86, 1694-1704 (1981).

[8] K. Stamnes, S. C. Tsay, W. Wiscombe and K. Jayaweera, “Numerically stable algorithm for discrete-ordinate-method radiative transfer in multiple scattering and emitting layered media,” Appl. Opt. 27, 2502-2509 (1988).

[9] M. I. Mishchenko, J. M. Dlugach, E. G. Yanovitskij and N. T. Zakharova, “Bidirectional reflectance of flat, optically thick particulate layers: an efficient radiative transfer solution and applications to snow and soil surfaces,” J Quant. Spectrosc. & Radiat. Transfer 63, 409-432 (1999).

[10] C. Bruegge, N. Chrien and D. Hanner, “A spectralon BRF data for MISR calibration applications,” Remote Sens. Environ. 76, 354-366 (2001).

[11] M. I. Mishchenko, L. D. Travis and A. A. Lacis, *Scattering, absorption and emissions by small particles* (Cambridge Univ., New York, 2002).